Journal of Non-Crystalline Solids 443 (2016) 91–96

Contents lists available at ScienceDirect

Journal of Non-Crystalline Solids

journal homepage: www.elsevier.com/locate/jnoncrysol

Preparation of Ni-based bulk metallic glasses with high corrosion resistance

Xu Ma [a], Ni Zhen [a], Junjiang Guo [a], Qiang Li [a,*], Chuntao Chang [b,*], Yanfei Sun [a]

[a] School of Physics Science and Technology, Xinjiang University, Urumqi, Xinjiang 830046, People's Republic of China
[b] Ningbo Institute of Materials Technology & Engineering, Chinese Academy of Sciences, Ningbo, Zhejiang 315201, People's Republic of China

ARTICLE INFO

Article history:
Received 5 January 2016
Received in revised form 7 April 2016
Accepted 10 April 2016
Available online 22 April 2016

Keywords:
Ni-based bulk metallic glasses
Glass forming ability
Corrosion properties
Mechanical properties

ABSTRACT

Bulk $Ni_{77-x-y}Mo_xCr_yNb_3P_{14}B_6$ (x = 7 y = 0; x = 8 y = 0; x = 9 y = 0; x = 5 y = 3; x = 5 y = 5; x = 5 y = 8; x = 8 y = 3; x = 8 y = 5, all in at.%) glassy alloy rods with the diameters of 1.0–1.5 mm were synthesized by combining fluxing technique and J-quenching technique. The effects of Mo and Cr substitution for Ni on the glass forming ability (GFA), thermal stability, mechanical properties and corrosion properties of the present Ni-based bulk metallic glasses (BMGs) had been studied systematically. It is found that the substitution of an appropriate amount of Cr and Mo for Ni can enhance the GFA of the present Ni-based alloys, while excessive substitution will lead to the degradation of the GFA. The corrosion tests show that the corrosion current density and corrosion rate of most of the present Ni-based BMGs in 1 M NaCl and 1 M HCl solutions are in the order of 10^{-6} A/cm^2 and 10^{-2} mm/year, respectively, exhibiting very high corrosion resistance. The addition of the appropriate Mo content and the Cr content as much as possible are benefit for the enhancement of the corrosion resistance of the present Ni-based BMGs. The compressive tests show that that the present Ni-based BMGs exhibit a compressive strength of 2.5–3.4 GPa, but nearly zero compressive plasticity.

1. Introduction

Due to unique atomic arrangement in comparison to crystalline counterpart, amorphous alloys exhibit many excellent properties, such as high mechanical strength, excellent magnetic properties and good corrosion resistance [1,2], and thus are attracting more and more attentions and becoming one of hot topics in the research of new materials in recent decades. Conventionally, an alloy can only be amorphized at a very high cooling rate. As a result, at least one dimension of the resultant amorphous alloys is very small, which has so far limited commercial applications of this class of materials. Through the efforts of many researchers, a large number of bulk metallic glasses (BMGs) such as La-, Zr-, Fe-, Co- and Ni-based alloys [3–6] have been successively developed in the past three decades. Among these BMGs, Ni-based BMGs usually exhibit high thermal stability, good mechanical properties and excellent corrosion resistance [5,7–9]. For instance, the fracture strength of $Ni_{59}Zr_{16}Ti_{13}Si_3Sn_2Nb_7$ can be reached 3 GPa and the plasticity can be reached 6.5% [10]. The corrosion rate of $(Ni_{60}Nb_{10}Ta_{30})_{0.95}P_5$ BMG in 12 M HCl solution determined by weight loss of the immersion test is almost zero [11]. However, at present most of the research on Ni-based BMGs has focused on all-metal Ni-based alloy systems, and only a few has focused on Ni-metalloid based alloy systems. This may be due to the low glass forming ability (GFA) of Ni-metalloid based alloys. Further, many of the recently reported Ni-metalloid based BMGs contain a considerable number of precious metal element Pd [12,13], which greatly increases the production cost of these Ni-based BMGs and thus limits their commercial application. So it is of both academic and industrial significance to develop new Ni-metalloid based BMGs.

At present the $Fe_{80}P_{13}C_7$ BMG with a maximum diameter of 2.0 mm has been synthesized by means of the combination method of fluxing treatment and J-quenching technique [14]. This reveals that J-quenching technique has unique advantages in the preparation of BMGs compared with the conventional copper mold casting technique, and thus provides us a great opportunity to develop new Ni-based BMGs. In addition, it is found that the suitable addition of some elements to metallic glasses may produce significant changes of their GFA, magnetic properties, mechanical properties and corrosion resistance [15–19]. For example, through the substitution of 6 at.% Fe by Mo in $Fe_{80}P_{13}C_7$ alloy, the critical diameter for fully glass formation of the alloy increases from 2 mm to 6 mm, and meantime the compressive fracture strength and plasticity of the BMG are also greatly improved [18]. The appropriate addition of Cr and Mo results in the effective enhancement of the corrosion resistance of $Fe_{80}P_{13}C_7$ amorphous alloy [19]. Based on the above considerations, a new series of $Ni_{77-x-y}Mo_xCr_yNb_3P_{14}B_6$ (x = 7 y = 0; x = 8 y = 0; x = 9 y = 0; x = 5 y = 3; x = 5 y = 5; x = 5 y = 8; x = 8 y = 3; x = 8 y = 5, all in at.%) BMGs has been developed, and the effects Mo and Cr contents on the GFA, corrosion resistance and

* Corresponding authors.
E-mail addresses: qli@xju.edu.cn (Q. Li), ctchang@nimte.ac.cn (C. Chang).

http://dx.doi.org/10.1016/j.jnoncrysol.2016.04.020
0022-3093/

mechanical properties of the present NiMoCrNbPB BMGs are studied systematically in this work.

2. Experimental procedure

$Ni_{77-x-y}Mo_xCr_yNb_3P_{14}B_6$ (x = 7 y = 0; x = 8 y = 0; x = 9 y = 0; x = 5 y = 3; x = 5 y = 5; x = 5 y = 8; x = 8 y = 3; x = 8 y = 5, all in at.%) master alloy ingots were prepared by torch-melting the mixtures of high-pure Ni powder (99.9 mass%), Cr powder (99.9 mass%), Mo powder (99.9 mass%), Boron particle (99.9 mass%), Niobium powder (99.9 mass%) and Ni_2P powder (99.5 mass%) in a clear fused silica tube under a high-purity argon atmosphere by a torch. Subsequently the *as*-prepared master alloy ingots were fluxed in a fluxing agent composed of B_2O_3 and CaO with the mass ratio of 3:1 at an elevated temperature for 4 h under a vacuum of ~50 Pa. After cooling down to room temperature, the alloy ingots were cleaned in an ultrasonic cleaner with absolute ethyl alcohol. Subsequently the alloy ingots were casted to be the alloy rods by J-quenching technique of which details can be found elsewhere [1]. As a result, $Ni_{77-x-y}Mo_xCr_yNb_3P_{14}B_6$ (x = 7 y = 0; x = 8 y = 0; x = 9 y = 0; x = 5 y = 3; x = 5 y = 5; x = 5 y = 8; x = 8 y = 3; x = 8 y = 5, all in at.%) alloy rods with the various diameters and the length of a few centimeters had been fabricated by J-quenching technique.

The glassy nature of the as-cast specimens was confirmed by X-ray diffraction (XRD, Bruker D2 PHASER) with Cu K α radiation (30 kV and 30 mA) at room temperature. The thermal behavior of the as-cast specimens was examined by differential scanning calorimetry (DSC, NETZSCH DSC 404F1) at a heating rate of 0.33 K/s under an Ar atmosphere. Electrochemical measurements were conducted in a three-electrode cell using a platinum counter electrode, a K/KCl reference electrode and a working electrode which is the as-prepared glassy alloy rod. Potentiodynamic polarization curves were measured with a potential sweep rate of 1 mV/s in both 1 M HCl and 1 M NaCl solutions open to air at room temperature after having immersed the specimens for about 20 min in order to make the open-circuit potential steady. The corrosion rates were evaluated from the weight loss after immersion for 1 week in 1 M NaCl solution at room temperature. Three specimens for each alloy in the same solution were examined for the weight loss test and the average value was used for corrosion rate estimation. Electrochemical impedance spectroscopy (EIS) of the specimens in both 1 M HCl and 1 M NaCl solutions was measured at room temperature using CS350 electrochemical workstation (Wuhan CorroTest Instrument Co. Ltd., China). EIS were recorded at open circuit potentials in the frequency ranging from 10^5 to 10^{-2} Hz, with a sinusoidal signal perturbation of 5 mV. The specimens held in the corrosion solutions at open circuit potential for 20 min to get a stationary open circuit potential before the test of EIS. Compressive tests of the specimens were performed on a testing machine (Reger, RGM-4100) at a strain rate of $5 \times 10^{-4}\ s^{-1}$ at room temperature. The compression specimens were prepared in the shape of cylindrical rods with a diameter of 1 mm and a length of 2 mm, and both end faces were polished carefully to ensure parallelism.

3. Results and discussion

Fig. 1 shows the XRD patterns of the *as*-cast $Ni_{77-x-y}Mo_xCr_yNb_3P_{14}B_6$ (x = 7 y = 0; x = 8 y = 0; x = 9 y = 0; x = 5 y = 3; x = 5 y = 5; x = 5 y = 8; x = 8 y = 3; x = 8 y = 5, all in at.%) glassy rod specimens with the maximum diameter (D_{max}). The XRD patterns of all the specimens reveal only a broad diffuse peaks and no apparent crystalline phase peaks, indicating that all the specimens just consist of a single glass phase at the sensitivity of XRD. When Ni is substituted solely by Mo in the $Ni_{77}Nb_3P_{14}B_6$ alloy, the bulk glassy alloy rods with the diameter of 1.0 mm can be prepared for the Mo substitution content of 7, 8 and 9 at.%, respectively. When the Mo content is fixed and Ni is further substituted by Cr in the present Ni-based alloys, the D_{max} of the obtained

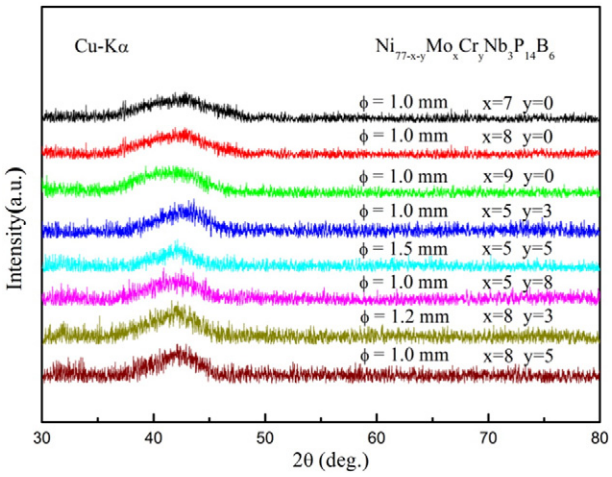

Fig. 1. XRD patterns of as-cast $Ni_{77-x-y}Mo_xCr_yNb_3P_{14}B_6$ glassy rod alloys with the corresponding maximum diameters for fully glass formation.

bulk glassy alloy rods are 1.0, 1.5 and 1.0 mm for the Mo content of 5 at.% and the Cr substitution content of 3, 5 and 8 at.%, respectively, and are 1.2 and 1.0 mm for the Mo content of 8 at.% and the Cr substitution content of 3 and 5 at.%, respectively. When the Mo and Cr contents are beyond the above range, the glassy alloy rod with a diameter larger than 1 mm cannot be obtained for the present Ni-based alloys in our experiment. It is indicated that the proper substitution of Mo and Cr for Ni can effectively enhance the GFA of the present Ni-based alloys. Based on Inoue's three principles for BMG formation [1], the larger negative heats of mixing among the constituent elements will facilitate the glass formation of alloy. The heats of mixing for Mo–P, Cr–P, Ni–P, Mo–B, Cr–B and Ni–B atomic pairs are −53.5, −49.5, −34.5, −34, −31 and −24 kJ/mol, respectively [20]. Therefore, the substitution of Mo and Cr for Ni will increase the average bond energy of the alloy and improve the stability of liquid phase, thus enhancing the GFA. Moreover, since the atomic sizes change in the order of Mo > Cr ≈ Ni > P > B [20], the substitution of Ni by Mo and Cr will lead to the wider atomic size distribution, which is favorable to increase the atomic packing density of the molten alloy. So this will improve the stability of liquid phase and increase the difficulty of the atomic rearrangement, thus leading to the enhancement of the GFA of the present Ni-based alloys [1]. Additionally, compared with the solely addition of Mo, the co-addition of Mo and Cr can more effectively enhance the GFA of the present Ni-based alloys. According to the "confusion principle" [21], the co-addition of Mo and Cr further increases the entropy and dense random packing of the molten alloy, thus leading to the enhancement of the GFA. However, it can be noted that the too much substitution content of Mo and Cr for Ni will degrade the GFA of the present Ni-based alloys. As mentioned previously, Mo and Cr have the larger negative enthalpy of mixing with the metalloid elements of P and B compared with Ni. Therefore, the excessive substitution of Mo and Cr for Ni could induce the formation of the Mo/Cr-contained intermediate phases in the molten alloy [18], which leads to the degradation of the GFA of the present Ni-based alloys.

Fig. 2 displays the DSC thermal scans for the *as*-cast $Ni_{77-x-y}Mo_xCr_yNb_3P_{14}B_6$ (x = 7 y = 0; x = 8 y = 0; x = 9 y = 0; x = 5 y = 3; x = 5 y = 5; x = 5 y = 8; x = 8 y = 3; x = 8 y = 5, all in at.%) glassy rod specimens at the heating rate of 0.33 K/s. All the specimens show a clear glass transition, followed by an extended supercooled liquid region and a single-stage crystallization process. The glass transition temperature (T_g), the onset crystallization temperature (T_x), the melting temperature (T_m), and the liquidus temperature (T_l) parameters (marked by arrows in Fig. 2) are summarized in Table 1. It can be seen that the T_g values of the present Ni-based BMGs increase with the total content of Mo and Cr. It is known that the T_g of amorphous alloys mainly depend on the atomic bonding strength between the constituent elements [22].

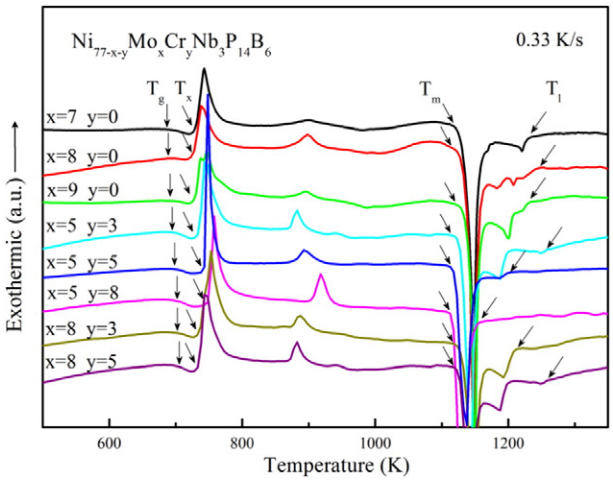

Fig. 2. DSC thermal scans of as-cast $Ni_{77-x-y}Mo_xCr_yNb_3P_{14}B_6$ glassy rod alloys at a heating rate 0.33 K/s.

The bond strength between atoms will be reflected by the enthalpy of mixing between them and the larger negative mixing enthalpy corresponds to the stronger bond strength. As mentioned before, the negative enthalpy of mixing for Mo/Cr-P and Mo/Cr-B atomic pairs are larger than that of Ni-P and Ni-B atomic pairs, respectively. So the substitution of Mo and Cr for Ni will result in the stronger bonding between the constituent elements of the present Ni-based BMGs, thus the higher T_g.

To further explore the effect of Mo and Cr contents on the GFA of the present Ni-based alloys, three common GFA parameters (the reduced glass transition temperature T_{rg} $(=T_g/T_l)$, the supercooled liquid region ΔT_x $(=T_x - T_g)$, and the parameter γ $(=\frac{T_x}{T_g+T_l})$) are calculated for the present Ni-based BMGs and listed in Table 1. It can be seen, except for the specimen with x = 5 y = 8, these three GFA parameters show relatively satisfactory correlations with the GFA, which refers to the experimental results of the D_{max}.

Fig. 3 shows the potentiodynamic polarization curves of the present Ni-based BMGs in 1 M HCl and 1 M NaCl solutions open to air at room temperature. The electrochemical parameters of the specimens including the corrosion potential (E_{corr}), corrosion current density (I_{corr}) and the corrosion rate (R_{corr}) calculated according to the I_{corr} are derived from the polarization curves and summarized in Table 2. The lower I_{corr} implies the better corrosion resistance. It can see that the I_{corr} of most of the present Ni-based BMGs is in the order of 10^{-6} A/cm^2, exhibiting the excellent corrosion resistance. The high corrosion resistance is firstly contributed to the structurally and chemically homogenous amorphous structure of the Ni-based BMGs, which results in a uniform and stable surface passive film which can protect the alloy against corrosion [23,24]. Moreover, Ni tends to form compact and stable passive layer during the corrosion process [25], which leads to the

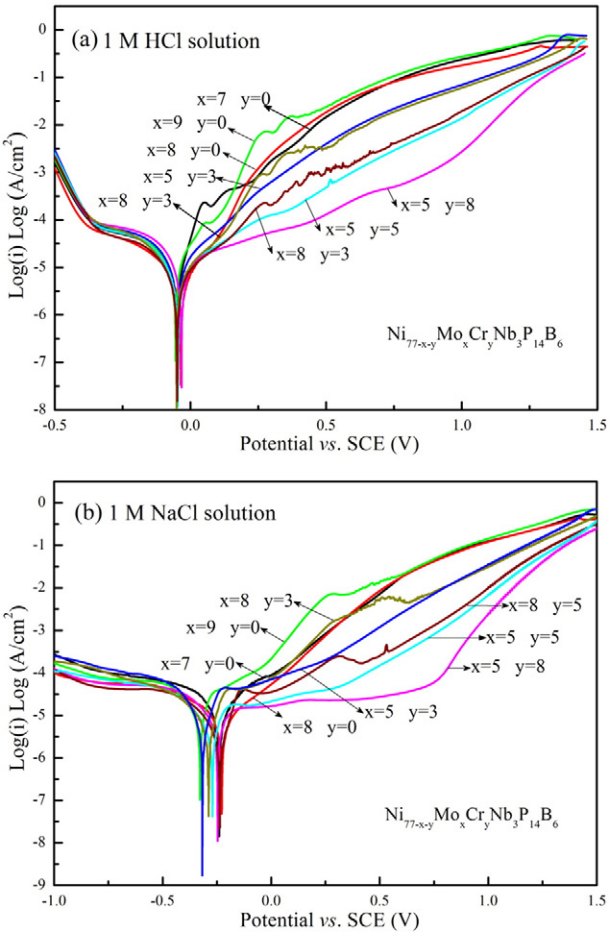

Fig. 3. Potentiodynamic polarization curves of the present Ni-based BMGs open to air at room temperature in 1 M HCl solution (a) and 1 M NaCl solution (b).

high corrosion resistance of Ni-based alloys. In the following, we first consider the case in the 1 M HCl solution. When Ni is individually replaced by Mo, the I_{corr} of the specimens firstly decreases and then increases with increasing the Mo substitution content from 7 at.% to 9 at.%, and reaches the minimum value at the Mo substitution content of 8 at.%. When the content of Mo is fixed at 5 at.% or 8 at.% and Ni is further substituted by Cr, the I_{corr} of the specimens increases continuously with the Cr substitution content. The results in 1 M NaCl solution are similar to those in 1 M HCl solution. It is known that both Mo and Cr are corrosion resistance elements and can form a stable passive film during the corrosion process, thus improving the corrosion resistance of the alloy [26,19]. Therefore, the addition of the appropriate amount of Mo leads to the improvement of corrosion resistance of the present Ni-based BMGs. However, it also indicates that the excessive addition

Table 1
Summary of the thermal parameters determined from the DSC curves and the mechanical properties of the present $Ni_{77-x-y}Mo_xCr_yNb_3P_{14}B_6$ BMGs (D_{max}: the critical diameters for fully glass formation; T_g: the glass transition temperature; T_x: the onset temperature of crystallization; T_m: the melt point; T_l: the liquid temperature; $T_{rg} = T_g/T_m$; $\Delta T_x = T_x - T_g$; $\gamma = T_x / (T_g + T_l)$; σ_f: compressive fracture strength, ε_p: plastic strain).

BMGs (at.%)	D_{max} (mm)	Thermal properties and the indicators of GFA							Mechanical properties	
		T_g (K)	T_x (K)	T_m (K)	T_l (K)	ΔT_x (K)	T_{rg}	γ	σ_f(GPa)	ε_f(%)
x = 7 y = 0	1.0	688	729	1144	1236	41	0.601	0.379	2.47 ± 0.16	0
x = 8 y = 0	1.0	691	729	1145	1247	38	0.603	0.376	2.52 ± 0.05	0
x = 9 y = 0	1.0	693	730	1143	1236	37	0.606	0.378	2.57 ± 0.04	0
x = 5 y = 3	1.0	694	746	1124	1263	52	0.617	0.381	2.60 ± 0.08	0
x = 5 y = 5	1.5	697	751	1124	1206	54	0.620	0.395	3.10 ± 0.05	0
x = 5 y = 8	1.0	699	752	1124	1161	53	0.622	0.404	3.11 ± 0.07	0
x = 8 y = 3	1.2	701	743	1140	1216	42	0.615	0.388	3.22 ± 0.06	0.3 ± 0.06
x = 8 y = 5	1.0	703	742	1139	1264	39	0.617	0.377	3.40 ± 0.17	0.1 ± 0.03

Table 2
Summary of the electrochemical parameters of the present $Ni_{77-x-y}Mo_xCr_yNb_3P_{14}B_6$ BMGs obtained from potentiodynamic polarization curves in 1 M HCl and 1 M NaCl solutions (E_{corr}: corrosion potential; I_{corr}: corrosion current density; R_{corr}: corrosion rate).

Solution	BMGs (at.%)	E_{corr} (mV)	I_{corr} (10^{-6} A/cm^2)	R_{corr} (mm/year)
1 M HCl solution	x = 7 y = 0	−0.050 ± 0.009	7.38 ± 0.609	0.057 ± 0.003
	x = 8 y = 0	−0.036 ± 0.157	3.49 ± 0.267	0.026 ± 0.005
	x = 9 y = 0	−0.055 ± 0.039	9.91 ± 0.762	0.078 ± 0.005
	x = 5 y = 3	−0.049 ± 0.033	3.35 ± 0.846	0.024 ± 0.001
	x = 5 y = 5	−0.047 ± 0.026	1.34 ± 0.399	$<10^{-3}$
	x = 5 y = 8	−0.033 ± 0.012	1.10 ± 0.342	$<10^{-3}$
	x = 8 y = 3	−0.051 ± 0.034	2.50 ± 0.631	0.019 ± 0.002
	x = 8 y = 5	−0.049 ± 0.0005	2.03 ± 0.101	0.015 ± 0.003
1 M NaCl solution	x = 7 y = 0	−0.244 ± 0.011	5.742 ± 0.210	0.163 ± 0.006
	x = 8 y = 0	−0.224 ± 0.029	4.641 ± 0.092	0.035 ± 0.001
	x = 9 y = 0	−0.328 ± 0.021	29.503 ± 1.021	0.223 ± 0.012
	x = 5 y = 3	−0.317 ± 0.006	3.394 ± 0.106	0.025 ± 0.004
	x = 5 y = 5	−0.259 ± 0.015	1.824 ± 0.117	0.014 ± 0.002
	x = 5 y = 8	−0.247 ± 0.027	1.685 ± 0.045	0.001 ± 0.001
	x = 8 y = 3	−0.288 ± 0.014	2.871 ± 0.032	0.022 ± 0.006
	x = 8 y = 5	−0.238 ± 0.003	2.385 ± 0.043	0.018 ± 0.002

of Mo leads to the degrading of the corrosion resistance of the present Ni-based BMGs. Many researches [27,19] have shown that the excess of Mo can cause the instability of chemical compound in the passive film of amorphous alloys, which causes the instability of passivation film and thus reduces the corrosion resistance of amorphous alloys. However Cr can form a stable passive film during corrosion process and its valence state does not change with the change of Cr content. Therefore, the higher Cr content leads to the thicker passivation film, thus the better corrosion resistance. Fig. 4 presents the corrosion rate of the present Ni-based BMGs determined from weight-loss measurement by immersing the specimens in 1 M HCl solutions open to air at room temperature for 168 h. The corrosion rate determined from weight-loss measurement as shown in Fig. 4 visually displays the corrosion resistance varied with the content of the present Ni-based BMGs, which is in good agreement with the corrosion rate calculated according to the I_{corr} as shown in Table 2 in both quality and quantity. The present Ni-based BMGs, especially $Ni_{67}Mo_5Cr_5Nb_3P_{14}B_6$ and $Ni_{64}Mo_5Cr_8Nb_3P_{14}B_6$ BMGs, exhibit a very low R_{corr} in the order of 10^{-2}–10^{-3} mm/year and a I_{corr} in the order of 10^{-6} A/cm^2 in both 1 M HCl and 1 M NaCl solutions. It is reported that Fe-Cr-Mo-(Nb, Ta)-CB BMGs exhibit a I_{corr} in the order of 10^{-3} A/cm^2 in 1 M HCl solution [28] and $Fe_{80-x}Ni_xP_{14}B_6$ (x = 20–50 at.%) BMGs exhibit a R_{corr} in the order of 10^{-1} mm/year and a I_{corr} in the order of 10^{-5} A/cm^2 in 1 M HCl solution [29]. It is indicated that the present Ni-based BMGs exhibit much higher corrosion resistance compared with Fe-based BMGs, which can be attributed to the uniform amorphous structure, the passive solvent element of Ni and the addition of the corrosion resistance elements of Cr and Mo.

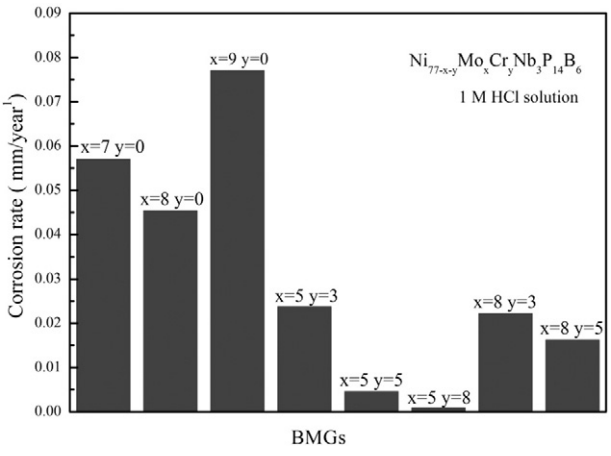

Fig. 4. The corrosion rate of the present Ni-based BMGs determined from weight-loss measurement by immersing the specimens in 1 M HCl solution open to air at room temperature for 168 h.

The Nyquist plots for the present Ni-based BMGs in 1 M HCl and 1 M NaCl solutions at room temperature are shown in Fig. 5. All the EIS plots as shown in Fig. 5(a) and (b) only consist of a single capacitance loop, and the corresponding equivalent circuit is shown in Fig. 5(c). The impedance data fitted from the equivalent circuit including the solution resistance (R_s), the polarization resistance (R_p), the magnitude of pure capacitor in absence of dispersive effect (Y_o) and the dispersion coefficient (n) are summarized in Table 3 [30]. The corrosion current density (I_{corr}) can be calculated from the impedance data by the following equation proposed by Diard et al. [31]:

$$I_{corr} = \frac{RT}{FnR_t} \tag{1}$$

where R is the gas constant, T the temperature, F the constant of Faraday. The calculated I_{corr} is also listed in Table 3. Larger R_p and smaller I_{corr} mean higher corrosion resistance. It can be seen that the result obtained from the EIS analysis is consistent with the results of the potentiodynamic polarization test and the weight-loss measurement in both quality and quantity.

Fig. 6 shows the room-temperature compressive stress-strain curves of as-cast glassy rod specimens with a diameter of 1.0 mm and a length of 2.0 mm. The fracture strength (σ_f) and the plastic strain (ε_p) of the specimens determined from the compressive stress-strain curves are listed in Table 1. The present Ni-based BMGs exhibit the relatively high fracture strength of 2.5–3.4 GPa. It is well known that the strength of BMGs can be universal scaling rule with the T_g because both the strength and T_g of amorphous alloys mainly depend on the atomic bonding strength among the constituent elements [32]. It can be seen from Table 1 that the σ_f of the present Ni-based BMGs change with composition is positively associated with their T_g, which follows the above scaling rule. Meanwhile, it can note that the reported fracture strength values of Fe-based BMGs are roughly around 3–4 GPa [33]. The T_g of Fe-based BMGs is around 700–900 K [33], and the T_g of the present Ni-based BMGs is 688–703 K. Therefore, it is understandable that the present Ni-based BMGs exhibit a relatively low compressive fracture strength as compared with Fe-based BMGs. In addition, the present Ni-based BMGs appear to have almost zero compressive plasticity. Recently it is suggested that the intrinsic plasticity of metallic glasses can be correlated with their elastic constants, such as the ratio of the shear modulus (G) to the bulk modulus (B) and the Poisson ration (ν), and the low G/B ratio and the high ν correspond to good ductility [33,

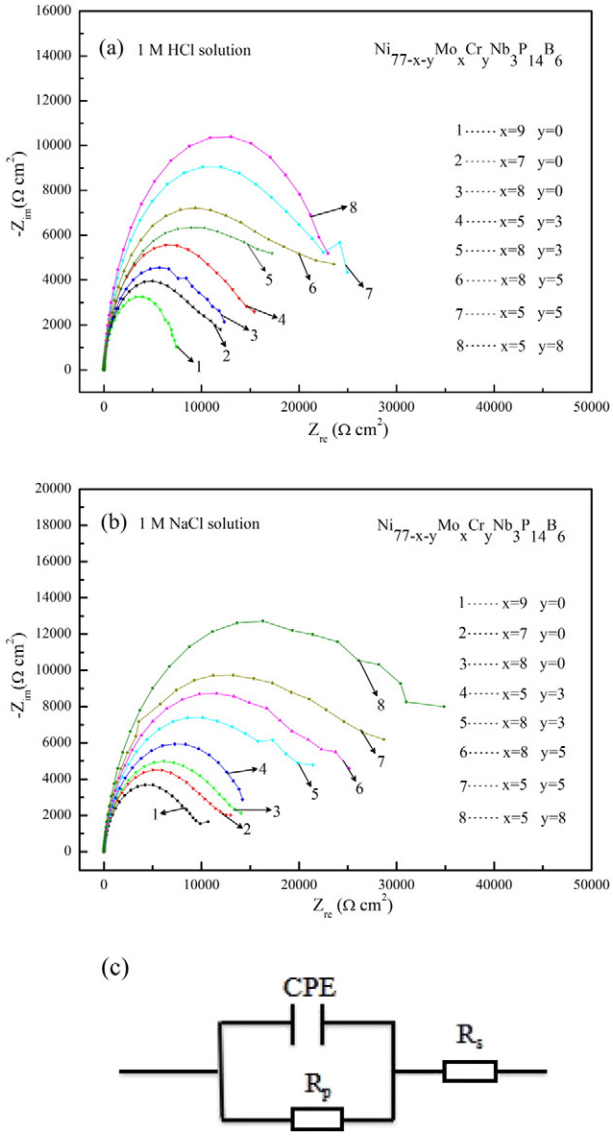

Fig. 5. Nyquist plots of the present Ni-based BMGs in 1 M HCl solution (a) and 1 M NaCl solution (b), and the equivalent circuit for the EIS plots (c).

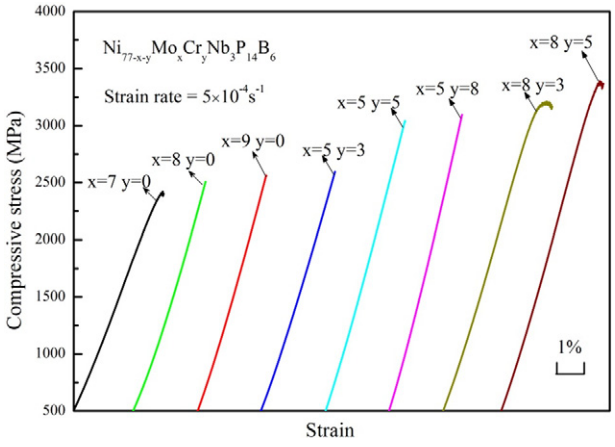

Fig. 6. Representative compressive stress–strain curves for the $Ni_{77-x-y}Mo_xCr_yNb_3P_{14}B_6$ bulk glassy alloy rods obtained at room temperature.

34]. Ni has a higher ν (0.31) and lower G/B ratio (0.42) compared to Fe [35]. As a result, the room-temperature plasticity of Fe-based BMGs is greatly enhanced through the substitution of Ni for Fe [29,36]. Therefore, from the above perspective, it can suggest that the ductility of Ni-based BMGs should be good, at least better than that of Fe-based BMGs. However, the present work does not support the above suggestion, indicating that the elastic constants are not the crucial and unique factor for the ductility of the present Ni-based BMGs. In fact, besides the constituent elements and the composition (which determine the weighted average of the elastic constants), the intrinsic mechanical properties of a BMG also depend on the atomic arrangement structure [35]. The further research is needed on this problem.

4. Conclusion

The new $Ni_{77-x-y}Mo_xCr_yNb_3P_{14}B_6$ (x = 7 y = 0; x = 8 y = 0; x = 9 y = 0; x = 5 y = 3; x = 5 y = 5; x = 5 y = 8; x = 8 y = 3; x = 8 y = 5, all in at.%) bulk glassy rod alloys have been successfully prepared by combining fluxing treatment and J-quenching technique in this study, and the critical diameter for fully glass formation reaches the maximum value of 1.5 mm at x = 5 y = 5. The present Ni-based BMGs exhibit the excellent corrosion resistance, and among the $Ni_{64}Mo_5Cr_8Nb_3P_{14}B_6$ BMG has the highest corrosion resistance with a I_{corr} in the order of

Table 3
The fitted results from EIS for the present Ni-based BMGs in 1 M HCl and 1 M NaCl solutions (R_s: solution resistance; R_p: polarization resistance; *CPE*: constant phase element; Y_o: magnitude of pure capacitor in absence of dispersive effect; n: dispersion coefficient; I_{corr}: corrosion current density calculated from the impedance data).

Solution	BMGs (at.%)	R_s (Ω cm^2)	R_p ($\times 10^4$ Ω cm^2)	*CPE*		I_{corr} (10^{-6} A cm^{-2})
				Y_0 ($\times 10^{-4}$ Ω S cm^2)	n	
1 M HCl solution	x = 7 y = 0	0.106	0.854	1.141	0.939	3.025
	x = 8 y = 0	0.119	1.180	1.138	0.940	2.181
	x = 9 y = 0	0.102	0.745	1.908	0.925	3.519
	x = 5 y = 3	0.111	1.01	1.562	0.930	2.583
	x = 5 y = 5	0.135	1.98	0.710	0.943	1.300
	x = 5 y = 8	0.122	2.38	1.056	0.921	1.107
	x = 8 y = 3	0.127	1.51	0.976	0.930	1.730
	x = 8 y = 5	0.103	1.66	1.822	0.889	1.646
1 M NaCl solution	x = 7 y = 0	0.367	1.041	1.124	0.900	2.589
	x = 8 y = 0	0.415	1.447	1.084	0.914	1.834
	x = 9 y = 0	0.346	0.803	1.279	0.926	3.262
	x = 5 y = 3	0.345	1.355	1.741	0.860	2.082
	x = 5 y = 5	0.428	1.819	0.744	0.926	1.440
	x = 5 y = 8	0.492	2.410	0.574	0.924	1.090
	x = 8 y = 3	0.315	1.808	1.367	0.867	1.549
	x = 8 y = 5	0.347	1.888	1.368	0.870	1.478

10^{-6} A/cm^2 and a $R_{corr} < 10^{-3}$ mm/year in both 1 M HCl and 1 M NaCl solutions. The present Ni-based BMGs exhibit the fracture strength of 2.5–3.4 GPa, but almost no compressive plasticity. The combination of the excellent corrosion resistance and relatively high strength, the present Ni-based BMGs show a promising application as advanced structural and functional materials in the future.

Acknowledgements

This research was sponsored by the National Natural Science Foundation of China (Grant No. 51261028 and 51561028).

References

[1] A. Inoue, Stabilization of metallic supercooled liquid and bulk amorphous alloys, Acta Mater. 48 (2000) 279–306.
[2] W.L. Johnson, Bulk glass-forming metallic alloys: science and technology, MRS Bull. 24 (1999) 42–56.
[3] A. Inoue, T. Zhang, Fabrication of bulk glassy $Zr_{55}Al_{10}Ni_5Cu_{30}$ alloy of 30 mm in diameter by a suction casting method, Mater. Trans. JIM 37 (1996) 185–187.
[4] T.D. Shen, R. Schwarz, Bulk ferromagnetic glasses prepared by flux melting and water quenching, Appl. Phys. Lett. 75 (1999) 49–51.
[5] H. Choi-Yim, D. Xu, W.L. Johnson, Ni-based bulk metallic glass formation in the Ni–Nb–Sn and Ni–Nb–Sn–X (X = B, Fe, Cu) alloy systems, Appl. Phys. Lett. 82 (2003) 1030–1032.
[6] A. Inoue, B.L. Shen, H. Koshiba, H. Kato, A.R. Yavari, Cobalt-based bulk glassy alloy with ultrahigh strength and soft magnetic properties, Nat. Mater. 2 (2003) 661–663.
[7] A. Kawashima, H. Habazaki, K. Hashimoto, Highly corrosion-resistant Ni-based bulk amorphous alloys, Mater. Sci. Eng. 304 (2001) 753–757.
[8] M. Lee, D. Bae, W. Kim, D. Kim, Ni-based refractory bulk amorphous alloys with high thermal stability, Mater. Trans. JIM 44 (2003) 2084–2087.
[9] J. Qiang, W. Zhang, A. Inoue, Formation and compression mechanical properties of Ni–Zr–Nb–Pd bulk metallic glasses, J. Mater. Res. 23 (2008) 1940–1945.
[10] M. Lee, J. Lee, D. Bae, W. Kim, D. Sordelet, D. Kim, A development of Ni-based alloys with enhanced plasticity, Intermetallics 12 (2004) 1133–1137.
[11] A. Kawashima, T. Sato, N. Ohtsu, K. Asami, Characterization of surface of amorphous Ni–Nb–Ta–P alloys passivated in a 12 kmol/m^3 HCl solution, Mater. Trans. JIM 45 (2004) 131–136.
[12] Y. Zeng, C. Qin, N. Nishiyama, A. Inoue, New nickel-based bulk metallic glasses with extremely high nickel content, J. Alloys Compd. 489 (2010) 80–83.
[13] A.I. Bazlov, A.Y. Churyumov, S.V. Ketov, D.V. Louzguine-Luzgin, Glass-formation and deformation behavior of Ni–Pd–P–B alloy, J. Alloys Compd. 619 (2015) 509–512.
[14] Q. Li, J.F. Li, P. Gong, K.F. Yao, J.E. Gao, H.X. Li, Formation of bulk magnetic ternary $Fe_{80}P_{13}C_7$ glassy alloy, Intermetallics 26 (2012) 62–65.
[15] L. Li, R. Liu, J. Zhao, H. Cai, Z. Yang, Effects of Nb addition on glass-forming ability, thermal stability and mechanical properties of ti-based bulk metallic glasses, Rare Metal Mater. Eng. 43 (2014) 1835–1838.
[16] X. Li, C. Qin, H. Kato, A. Makino, A. Inoue, Mo microalloying effect on the glass-forming ability, magnetic, mechanical and corrosion properties of $(Fe_{0.76}Si_{0.096}B_{0.084}P_{0.06})_{100-x}Mo_x$ bulk glassy alloys, J. Alloys Compd. 509 (2011) 7688–7691.
[17] T. Bitoh, D. Watanabe, Effect of yttrium addition on glass-forming ability and magnetic properties of Fe–Co–B–Si–Nb bulk metallic glass, Metals 5 (2015) 1127–1135.
[18] X.H. Yang, X.H. Ma, Q. Li, S.F. Guo, The effect of Mo on the glass forming ability, mechanical and magnetic properties of FePC ternary bulk metallic glasses, J. Alloys Compd. 554 (2013) 446–449.
[19] M.W. Tan, E. Akiyama, H. Habazaki, A. Kawashima, K. Asami, K. Hashimoto, The role of chromium and molybdenum in passivation of amorphous Fe-Cr-Mo-P-C alloys in deaerated 1 M HCl, Corros. Sci. 38 (1996) 2137–2151.
[20] A. Takeuchi, A. Inoue, Classification of bulk metallic glasses by atomic size difference, heat of mixing and period of constituent elements and its application to characterization of the main alloying element, Mater. Trans. JIM 46 (2005) 2817–2829.
[21] A.L. Greer, Confusion by design, Nature 366 (1993) 303–304.
[22] H.S. Chen, Glassy metals, Rep. Prog. Phys. 43 (1980) 353.
[23] S.J. Pang, T. Zhang, K. Asami, A. Inoue, Synthesis of Fe–Cr–Mo–C–B–P bulk metallic glasses with high corrosion resistance, Acta Mater. 50 (2002) 489–497.
[24] K. Leinartas, M. Samulevičien, A. Bagdonas, R. Juškenas, E. Juzeliūnas, Structural and anticorrosive properties of magnetron-sputtered Fe–Cr–Ni and Fe–Cr–Ni–Ta alloy films, Surf. Coat. Technol. 168 (2003) 70–77.
[25] J. Jayaraj, Y.C. Kim, K.B. Kim, H.K. Seok, E. Fleury, Corrosion behaviors of $Fe_{45-x}Cr_{18}Mo_{14}C_{15}B_6Y_2M_x$ (M = Al, Co, Ni, N and x = 0.2) bulk metallic glasses under conditions simulating fuel cell environment, J. Alloys Compd. 434 (2007) 237–239.
[26] M. Naka, K. Hashimoto, T. Masumoto, Effect of addition of chromium and molybdenum on the corrosion behavior of amorphous Fe-20B, Co-20B and Ni-20B alloys, J. Non-Cryst. Solids 34 (1979) 257–266.
[27] K. Asami, M. Naka, K. Hashimoto, T. Masumoto, Effect of molybdenum on the anodic behavior of amorphous Fe-Cr-Mo-B alloys in hydrochloric acid, J. Electrochem. Soc. 127 (1980) 2130–2138.
[28] S. Pang, T. Zhang, K. Asami, et al., New Fe-Cr-Mo-(Nb, Ta)-CB glassy alloys with high glass-forming ability and good corrosion resistance, Mater. Trans. 42 (2001) 376–379.
[29] L. Zhang, X.H. Ma, Q. Li, J.J. Zhang, Y.Q. Dong, C.T. Chang, Preparation and properties of $Fe_{80-x}Ni_xP14B6$ bulk metallic glasses, J. Alloys Compd. 608 (2014) 79–84.
[30] C.N. Cao, Corrosion Electrochemistry, Chemical Industrial Press, Beijing, 1994.
[31] J.P. Diard, B. Le Gorrec, C. Montella, J. Electrochim. Chem. 326 (1992) 13–36.
[32] J.J. Lewandowski, W.H. Wang, A. Greer, Intrinsic plasticity or brittleness of metallic glasses, Philos. Mag. Lett. 85 (2005) 77–87.
[33] C. Suryanarayana, A. Inoue, Iron-based bulk metallic glasses, Int. Mater. Rev. 58 (2013) 131–166.
[34] Y. Liu, H. Wu, C.T. Liu, Z. Zhang, V. Keppens, Physical factors controlling the ductility of bulk metallic glasses, Appl. Phys. Lett. 93 (2008) 151915.
[35] Y.Q. Cheng, A.J. Cao, E. Ma, Correlation between the elastic modulus and the intrinsic plastic behavior of metallic glasses, the roles of atomic configuration and alloy composition, Acta Mater. 57 (2009) 3253–3267.
[36] X.H. Ma, X.H. Yang, Q. Li, S.F. Guo, Quaternary magnetic FeNiPC bulk metallic glasses with large plasticity, J. Alloys Compd. 577 (2013) 345–350.